Adaptive behavior of bacterial mechanosensitive channels is coupled to membrane mechanics

Vladislav Belyy, Kishore Kamaraju, Bradley Akitake, Andriy Anishkin, and Sergei Sukharev

Department of Biology, University of Maryland, College Park, MD 20742

Mechanosensitive channel of small conductance (MscS), a tension-driven osmolyte release valve residing in the inner membrane of *Escherichia coli*, exhibits a complex adaptive behavior, whereas its functional counterpart, mechanosensitive channel of large conductance (MscL), was generally considered nonadaptive. In this study, we show that both channels exhibit similar adaptation in excised patches, a process that is completely separable from inactivation prominent only in MscS. When a membrane patch is held under constant pressure, adaptation of both channels is manifested as a reversible current decline. Their dose–response curves recorded with 1–10-s ramps of pressure are shifted toward higher tension relative to the curves measured with series of pulses, indicating decreased tension sensitivity. Prolonged exposure of excised patches to subthreshold tensions further shifts activation curves for both MscS and MscL toward higher tension with similar magnitude and time course. Whole spheroplast MscS recordings performed with simultaneous imaging reveal activation curves with a midpoint tension of 7.8 mN/m and the slope corresponding to ~15-nm^2 in-plane expansion. Inactivation was retained in whole spheroplast mode, but no adaptation was observed. Similarly, whole spheroplast recordings of MscL (V23T mutant) indicated no adaptation, which was present in excised patches. MscS activities tried in spheroplast-attached mode showed no adaptation when the spheroplasts were intact, but permeabilized spheroplasts showed delayed adaptation, suggesting that the presence of membrane breaks or edges causes adaptation. We interpret this in the framework of the mechanics of the bilayer couple linking adaptation of channels in excised patches to the relaxation of the inner leaflet that is not in contact with the glass pipette. Relaxation of one leaflet results in asymmetric redistribution of tension in the bilayer that is less favorable for channel opening.

INTRODUCTION

In all existing organisms, the envelopes surrounding cells are multilayer assemblies involving the bilayer cytoplasmic membrane, the underlying cytoskeleton, and the extracellular matrix or cell wall. Any mechanical perturbation of the cell envelope would involve reactions of all three elements and relaxation/remodeling processes that may occur at different spatial and time scales. The resultant stress in the lipid bilayer may depend on many factors, such as boundary conditions, initial membrane area excess, distribution and spontaneous curvature of the lipid constituents, as well as the degree of coupling between the inner and outer leaflets. Activities of mechanosensitive channels directly gated by tension in the lipid bilayer (Sachs and Morris, 1998; Hamill and Martinac, 2001) depend on all these interactions.

In a typical patch clamp experiment, a transversal pressure gradient applied to the patch sealed to a glass pipette is expected to stretch the entire multilayer membrane assembly. The stress should be shared between the bilayer and other stress-bearing elements (Wan et al., 1999; Zhang et al., 2000; Suchyna et al., 2009). The readout of such an experiment is often a transiently spiked mechano-activated current. The decay may not only reflect the adaptive process in the channel itself, but also changes in the stimulus perceived by the channel due to gradual stress redistribution in the assembly. Thus, the simple Young–Laplace pressure-to-tension conversion based on the apparent patch curvature and the pressure gradient does not necessarily reveal the true stimulus acting on individual channels. Even if the membrane of an excised patch is free of cytoskeleton and cell wall, the simple notion that only the outer leaflet is sealed to the glass pipette while the inner leaflet may be loosely coupled to the outer leaflet through the common membrane midplane raises the possibility that the tension distribution in this configuration could be asymmetric and time dependent (Baoukina and Mukhin, 2004). Correspondingly, under asymmetric stress in the lipid bilayer, the inner and outer rims of membrane-embedded channels may be subjected to different tensions. Stress relaxation/redistribution in the membrane may involve lipid exchange between the leaflets, viscous flow, and small-scale lipid rearrangements. Parameters that can potentially modulate such relaxation include

Correspondence to Sergei Sukharev: sukharev@umd.edu

Abbreviations used in this paper: DIC, differential interference contrast; MscL, mechanosensitive channel of large conductance; MscS, mechanosensitive channel of small conductance.

The Rockefeller University Press $30.00
J. Gen. Physiol. Vol. 135 No. 6 641–652
www.jgp.org/cgi/doi/10.1085/jgp.200910371

the total area of the stressed membrane, its protein content, and the distance of the region in question from the edge of the bilayer. The dependency of mechanosensitive channel activity and adaptation on patch configuration, presence of cytoskeleton, stimulation protocols, and voltage was reported for *Xenopus* oocytes (Hamill and McBride, 1992; Zhang et al., 2000), astrocytes (Suchyna et al., 2004), normal and dystrophic myotubes (Suchyna and Sachs, 2007), as well as cloned TREK-1 channels (Honoré et al., 2006).

The *Escherichia coli* mechanosensitive channels of small and large conductance (MscS and MscL, respectively) act as tension-driven osmolytic release valves, both residing in the bacterium's cytoplasmic (inner) membrane (Blount et al., 1996; Levina et al., 1999). MscL opens at lytic tensions in emergency situations, whereas MscS acts at tensions half as intense and appears to regulate turgor during the normal life cycle. The transient character of MscS gating was noticed even before its molecular identification (Koprowski and Kubalski, 1998) and confirmed immediately upon cloning (Levina et al., 1999). The complex adaptive behavior of MscS observed in patch clamp experiments involves processes previously termed "desensitization" and "inactivation" (Akitake et al., 2005). Desensitization manifests itself both as a gradual activation curve shift toward higher pressures (mode shift) and as an adaptive current decline when an excised patch is subjected to a prolonged stimulus of constant pressure. In contrast, inactivation refers to a tension-insensitive, nonconductive state that desensitized channels enter gradually if tension persists. An adaptive current decline was reported previously for liposome-reconstituted MscL as well (Häse et al., 1995). To adhere to the conventional terminology, the reversible current decline under sustained stimulation, or shifts of activation curve toward higher tension, will be called "adaptation." Adapted channels can be reactivated by a stronger stimulus. Channels that enter nonconductive and completely tension-insensitive states will be referred to as "inactivated."

Here, we show that reversible adaptation previously called desensitization (Akitake et al., 2005, 2007a) is not unique to MscS, but occurs in the structurally unrelated channel MscL under similar stimulation protocols in native patches excised from giant *E. coli* spheroplasts. The fact that the two channels exhibit very similar time courses of adaptation suggests that the process originates in a place other than the molecule itself, most likely the lipid bilayer. Switching to a whole spheroplast or intact spheroplast-attached recording configuration reveals a complete absence of adaptive current decline in MscS and MscL, in striking contrast to the channel's behavior in excised patches. Given that geometry and size of the membrane are the only difference between the two recording modes, we propose that the process of adaptation is directly linked with stress relaxation specifically in excised patches.

MATERIALS AND METHODS

Electrophysiology

Wild-type MscS channels were expressed in MJF465 cells (Levina et al., 1999) and pB113 cells (Li et al., 2002) from the pB10b vector (Okada et al., 2002). Preparation of giant *E. coli* spheroplasts and patch-clamping procedures were conducted as described previously (Blount et al., 1999; Akitake et al., 2005). Population channel recordings were conducted on excised inside-out patches, cell-attached patches, and in whole spheroplast mode in symmetrical buffers containing 200 mM KCl, 10 mM $CaCl_2$, 40 mM $MgCl_2$, and 10 mM HEPES, pH 7.4. The bath solution differed only in the addition of 400 mM sucrose. Traces were recorded using Clampex 10.2 software (MDS Analytical Technologies). Mechanical stimuli were delivered using a high-speed pressure clamp apparatus (HSPC-1; ALA Scientific Instruments) equipped with a more powerful custom-made suction pump providing 10-ms raise time to 300 mmHg. To obtain spheroplast-attached recordings, after seal formation the cell was left unperturbed and mechanosensitive currents were invoked by applying negative pressure (suction) as in excised patches. When the spheroplast membrane remained intact, individual channel conductances were noticeably smaller than normal due to the series resistance of the cell membrane.

In whole spheroplast recording mode, the pipette-facing membrane of the patched spheroplast was removed by delivering a 0.5–5-ms high-voltage pulse through the patch clamp amplifier's "zap" function (Axopatch 200B; Axon Instruments). The spheroplasts used in whole cell experiments had not been induced with isopropyl β-D-1-thiogalactopyranoside and expressed channel at reduced density only due to promoter leakage, and yet the whole cell currents at +30 mV approached 5–7 nA. Attempts to record from induced spheroplasts led to an overload of the amplifier. The channels were mechanically stimulated by ramps or steps of positive pressure. Traces were corrected for serial resistance, normalized to the conductance at saturating pressure $g_n = g/g_{sat}$, and the dose–response curves ($g_n(\gamma)$) were fitted to the Boltzmann-type equation $g_n = 1/(1+\exp(\Delta E - \gamma \Delta A)/kT)$, where γ is membrane tension, ΔE is the energy difference between the closed and open states at rest, and ΔA is the in-plane area expansion of the protein.

Imaging and analysis

Recording MscS currents in whole spheroplast mode allowed us to determine the channel's open probability and midpoint tension. Measurements of the spheroplast's radius at the midpoint pressure ($p_{0.5}$) were done by direct imaging under increasing pressure gradient. Pressures were then converted into tensions by applying the law of Laplace. Spheroplasts were imaged continuously under differential interference contrast (DIC) at a rate of 30 frames per second during the application of a 1-s saturating ramp. To determine the radius of curvature, the images of cells corresponding to the lowest, highest, and approximately $p_{0.5}$ MscS pressure levels were fit to a circle by placing a set of points at the spheroplast boundary in a MATLAB script (The MathWorks, Inc.). Based on the properties of DIC optics (Young et al., 1998), the edge of the spheroplast was visually determined to lie at the outermost boundary between the background gray and the shifted intensity of the spheroplast; i.e., the gray–black interface on one side of the cell and the gray–white interface on the other.

Online supplemental material

Fig. S1 shows the behavior of the MscS population in an excised patch under fast ramp stimulation, which suggested 1-s linear ramps as a "standard" midpoint characterization protocol used throughout the study. Fig. S2 illustrates the asymmetry and hysteresis of MscS and MscL population currents in response to symmetric triangular ramps of pressure. Fig. S3 shows that under a 1-s

triangular ramp, hysteresis in MscS is also observed in the whole spheroplast mode. Fig. S4 illustrates a distinction between the adaptive MscS current decline observed in excised patches and channel inactivation, as the two processes have opposite tension dependencies. Figs. S1–S4 are available at http://www.jgp.org/cgi/content/full/jgp.200910371/DC1.

RESULTS

Adaptive behavior of MscS and MscL in excised patches

Fig. 1 (A and B) shows pairs of activation curves for MscS and MscL, one of which is a continuous trace recorded under a 1-s linear ramp of pressure, and the other is reconstructed from the discrete peak currents recorded in response to a series of machine-limited pulses (10 ms raise time). For the ramp response, the midpoint was determined as the pressure at which instantaneous current was half of the current at saturation. The midpoint for the pulse-based curve was determined from the two-state Boltzmann fit. The 23-mmHg shift between the two curves indicates that gradually applying tension with a 1-s ramp decreases the efficiency of tension stimuli by about one fifth. Statistics obtained from six independent patches gave a value of 19 ± 7% for average midpoint shift from the pulse-based to ramp-based activation curves for MscS. Both channels' dose–response curves recorded with saturating pressure ramps are always right-shifted relative to the curves measured with pulses, indicating that either both types of channels subjected to tension possess similar inherent time-dependent tension sensitivity or the mechanical stimulus reaching them through the membrane declines with time and is somehow different in these two protocols.

Choosing the stimulus ramp length in the above experiment was based upon several tests. We recorded activation curves at increasing ramp speed, with the steepest being a machine-limited 10-ms "pulse" (Fig. S1). Short ramps (<100 ms) elicited activation curves with higher pressure midpoints ($p_{0.5}$), apparently due to the combined viscosity in the pneumatic system and kinetic

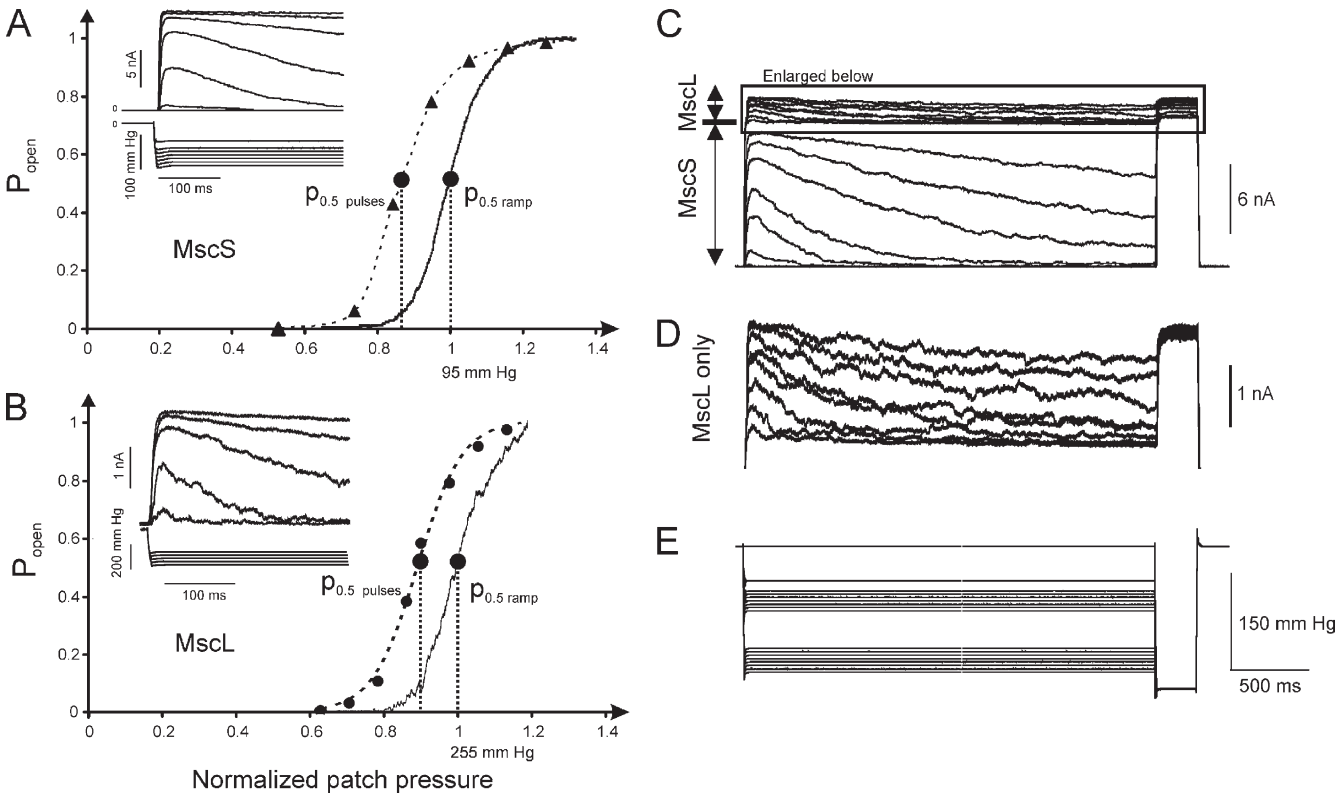

Figure 1. MscS and MscL adapt when expressed in *E. coli* spheroplasts separately or together. (A and B) A comparison of dose–response curves taken with a series of pressure steps and a 1-s linear ramp from 0 to saturating pressure. Pairs of dose–response curves are shown for MscS (A) and MscL (B) individually expressed in MJF465 spheroplasts. Insets show current responses of the excised patch to the series of pressure steps, with a machine-limited 10-ms raise time. The ramp-generated curves are always right-shifted by 10–20% on the pressure scale. For MscS (A), maximal current was 1.4 nA and ramp $p_{0.5}$ = 95 mmHg. For MscL (B), saturating current was 3.14 nA and $p_{0.5}$ = 255 mmHg with the ramp stimulus. (C–E) MscS and MscL show similar tension- and time-dependent decline of currents when coexpressed in PB113 spheroplasts carrying a native copy of the *mscL* gene. Both channels were probed with 3-s pressure steps of varying amplitude. MscS activates in the lower range of pressures (C), whereas MscL (D) had to be probed with pressures twice as high, as seen from the pressure protocol (E). At pressures beyond 150 mmHg, MscS current completely saturates and MscL currents were recorded on top of a flat MscS response. As seen from the coinciding responses to saturating pulse (D), the inactivation of MscS and MscL after 3-s stimulation is negligibly small.

delays in channel response. As the ramp length increases beyond 250 ms, $p_{0.5}$ in the given patch stabilizes at 120 mmHg. We also found that with ramps longer than 5 s, the final current level progressively decreases, which can be ascribed to channel inactivation (Akitake et al., 2005). Based on these data, 1-s ramps were chosen as the preferred stimulus for measuring channel activation, as the population response in this regimen is not visibly limited by channel opening kinetics and the effect of inactivation along the ramp is negligible.

Using triangular ramps, we compared responses to ascending and descending stimuli. With longer ramps, we detected midpoint deviations from those observed under standard conditions (1-s ramp). Fig. S2 shows MscS and MscL population responses to saturating ascending and descending pressure ramps of different length. Ramps shorter than 1 s invariably result in the midpoints of both MscS and MscL being lower on the descending leg of the ramp than on the ascending leg. As ramp length is increased, the midpoint pressure on the descending leg of the ramp (closing direction) "catches up" and eventually surpasses the opening midpoint pressure. In four independent patches, the $p_{0.5}$ (opening)/$p_{0.5}$ (closing) ratio of MscS channels on 1-s ramps was found to be 17 ± 7% higher than that on 20-s ramps. Hysteresis is apparently kinetic in nature and can be explained by a relatively slow closing rate and opposite character of tension dependencies for the opening and closing rates.

Many studies described dependencies of MscS adaptation kinetics on pressure (Koprowski and Kubalski, 1998; Akitake et al., 2005, 2007a), voltage (Vasquez and Perozo, 2004; Akitake et al., 2005), presence of cosolvents (Grajkowski et al., 2005), or amphipathic agents (Akitake et al., 2007b; Kamaraju and Sukharev, 2008). It was unclear whether the adaptive mode shift is an intrinsic property of MscS specifically. Here, we found that both MscS and MscL are characterized by very similar adaptive behaviors while differing in their ability to inactivate. To observe both channels in the same patch, we expressed MscS in the *mscL*-positive PB113 strain. Repeated ramp experiments indicated that the midpoint

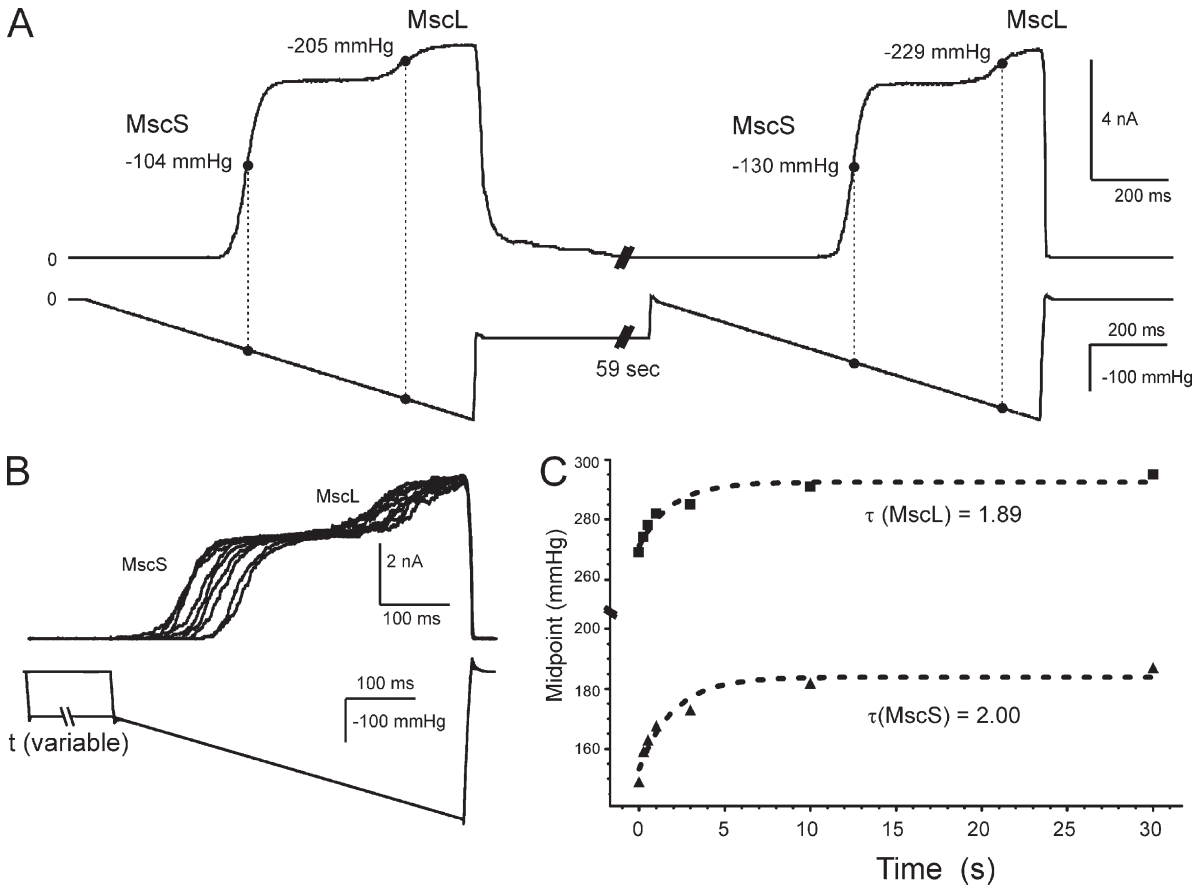

Figure 2. MscS and MscL both adapt, displaying similar right shifts of activation curves with similar time courses. (A) A pressure ramp response of an excised patch containing both MscS and MscL, followed by a prolonged (59-s) step of subthreshold pressure with a repeated ramp in the end. The midpoints scored with the second ramp are noticeably higher. (B) Superimposed traces in response to a 500-ms ramp show that the midpoint shift for both channels increases gradually with the duration of the subthreshold step varied between 0.2 and 59 s. (C) Plot of activation midpoints as a function of intervening step duration. The midpoints for MscS (bottom) and MscL (top) change concomitantly with characteristic times of ~2 s.

of MscL is 1.8 ± 0.1 (n = 13) times higher than that of MscS (~14 dynes/cm vs. ~7.8 dynes/cm on 1-s ramps). Because the midpoints are well separated, we were able to probe each population individually and show that the MscL current declines adaptively with nearly the same magnitude and time course as that of MscS. As shown in Fig. 1 C, at the end of each 3-s trace, the channel population was probed by a saturating pressure pulse, which evoked full population current with negligible deviations due to inactivation and demonstrated that the observed current decline was not a consequence of inactivation. Although MscL adaptation has previously been reported in liposomes (Häse et al., 1995), Fig. 1 (B and D) provides evidence for it in native bacterial membranes, and coexpression now allows us to compare the adaptive properties of MscS and MscL side by side. Adaptive current decline appears as partial loss of tension sensitivity, which is why the process was previously called "desensitization" or "mode shift" (Akitake et al., 2005, 2007a). As will be discussed below, the term "adaptation" describes adaptation of the stimulus rather than channel transition to a different state.

Ramp responses in patches containing both wild-type MscS and MscL are shown in Fig. 2 A. The two channels' midpoints shift toward higher pressures by nearly the same amount after a 1-min exposure to a subthreshold pressure step. Because MscL activates at substantially higher pressures than does MscS, the two populations produce a trace with two well-separated activation "waves." The curve shift in both channel populations was similar in pressure units, but when measured as a ratio of the naive midpoint it was more pronounced in MscS. In six independent patches, the midpoint shift of MscS varied between 15 and 25 mmHg after a 59-s preconditioning stimulus, whereas the midpoint shift of MscL varied between 10 and 20 mmHg.

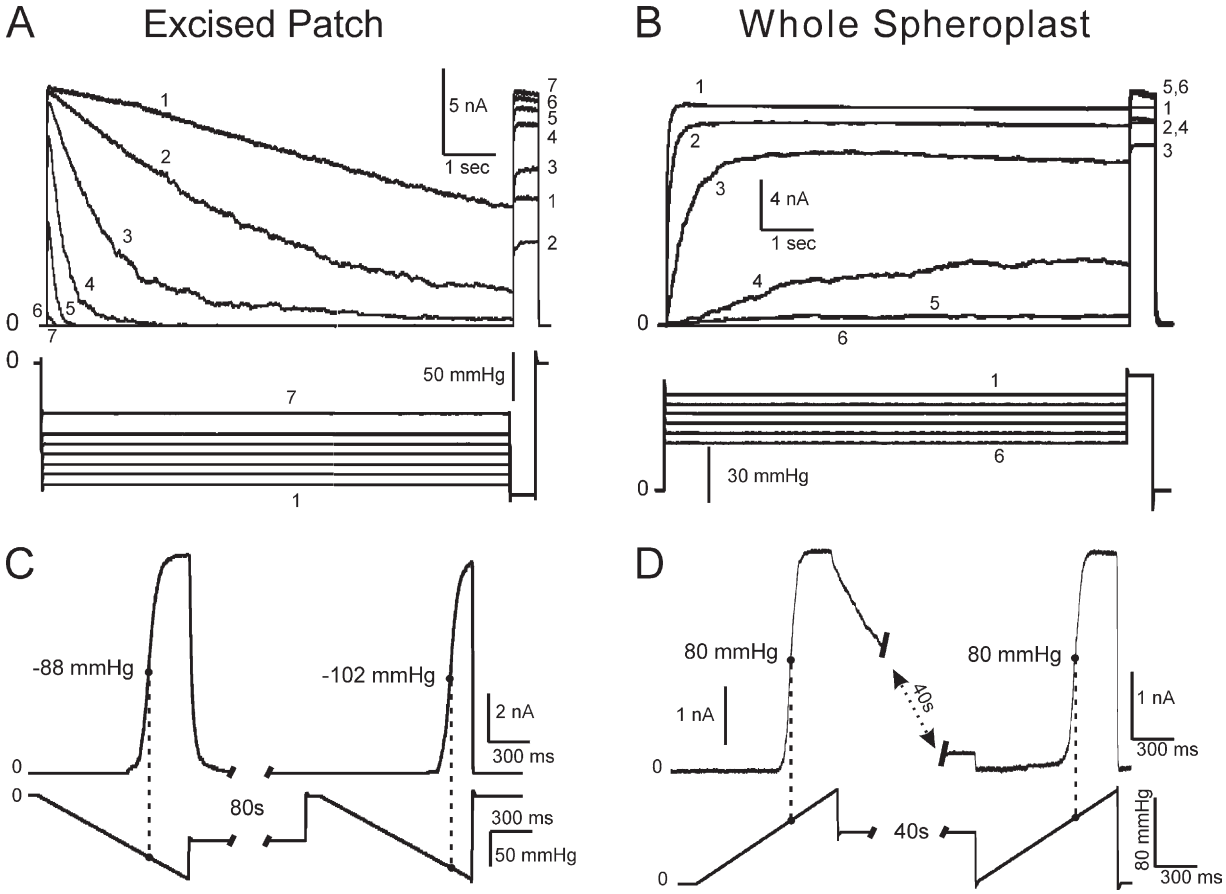

Figure 3. MscS adaptation is absent in whole spheroplast recording configuration. A typical dataset recorded in an excised patch illustrating adaptation: (A) current decay as a result of adaptation and (C) a substantial (~16%) midpoint shift in an experiment with two ramps separated by an 80-s step of subthreshold pressure. In the first case, a short (0.5-s) saturating test pulse was applied to the patch at the end of the step to reveal the non-inactivated fraction of the channel population. (B and D) A similar dataset obtained in whole spheroplast recording mode under steps or ramps of positive pressure. The responses to sustained pressure steps recorded on the same entire spheroplast show no current decay, yet the saturating pressure pulse at the end reveals that part of the population enters a tension-insensitive inactivated state (B). The two saturating ramps separated by a 40-s step of subthreshold pressure display identical responses with the same midpoint (D). In A and B, channels were stimulated with a 9-s step of intermediate pressure, followed by a 0.5-s saturating test pulse.

The conditioning subthreshold stimulus duration that affects MscS and MscL's mode shift was determined by subjecting a patch containing both channels to a subthreshold pressure for varying periods of time and testing the midpoints with identical 500-ms ramps before and after the stimulus (Fig. 2 B). The two channels' midpoints were plotted as a function of the conditioning stimulus duration (Fig. 2 C). Fitted with single-exponential functions, this dataset yielded remarkably similar characteristic times (τ = 1.89 s for MscL and 2.00 s for MscS). The two channel species share no homology, bear no structural resemblance, and have very different gating parameters. We conclude that the mechanosensitive channels MscS and MscL undergo simultaneous mode shift similar in amplitude and time course not because of a specific property prebuilt in their structure, but rather due to some type of stress redistribution in the patch membrane, the common environment for both of them.

Adaptation of MscS is absent in the whole spheroplast configuration

The whole cell mode was reproducibly achieved with intact spheroplasts after seal formation by "zapping" the patch with a brief electric pulse while applying slightly positive pipette pressure (5–7 mmHg). To compare the response of MscS in whole cells versus excised patches, we used identical stimulus protocols with ramps and steps, with one exception: in whole cell recordings, pipette voltage and pressure were inverted to accommodate for the inverse membrane orientation (Fig. 3). Although adaptation was absent in whole cell mode at all pressure levels, inactivation was clearly revealed by the two-step protocol. The current shown in Fig. 3 B does not decline over the course of the 9-s subsaturating step, but the saturating pulse in the end shows a decreased fraction of active channels, meaning that some inactivation had taken place. Note that inactivation is less pronounced in the whole cell mode (Fig. 3 B) compared with excised patches where the channels gradually close (Fig. 3 A). In both cases, the inactivated fraction depends non-monotonously on applied tension (see the numbers by the traces designating the order of applied pulses). It has been suggested previously that inactivation proceeds only from the closed or closed-adapted state (Akitake et al., 2007a), and that although the closed-to-inactivated transition rate increases with tension, only the closed channels are available for inactivation. Thus, increasing tension "locks" a progressively larger fraction of channels in the open state, from which they cannot inactivate. As a result, deeper inactivation is achieved in excised patches, where adaptation provides a larger pool of closed channels at a given tension.

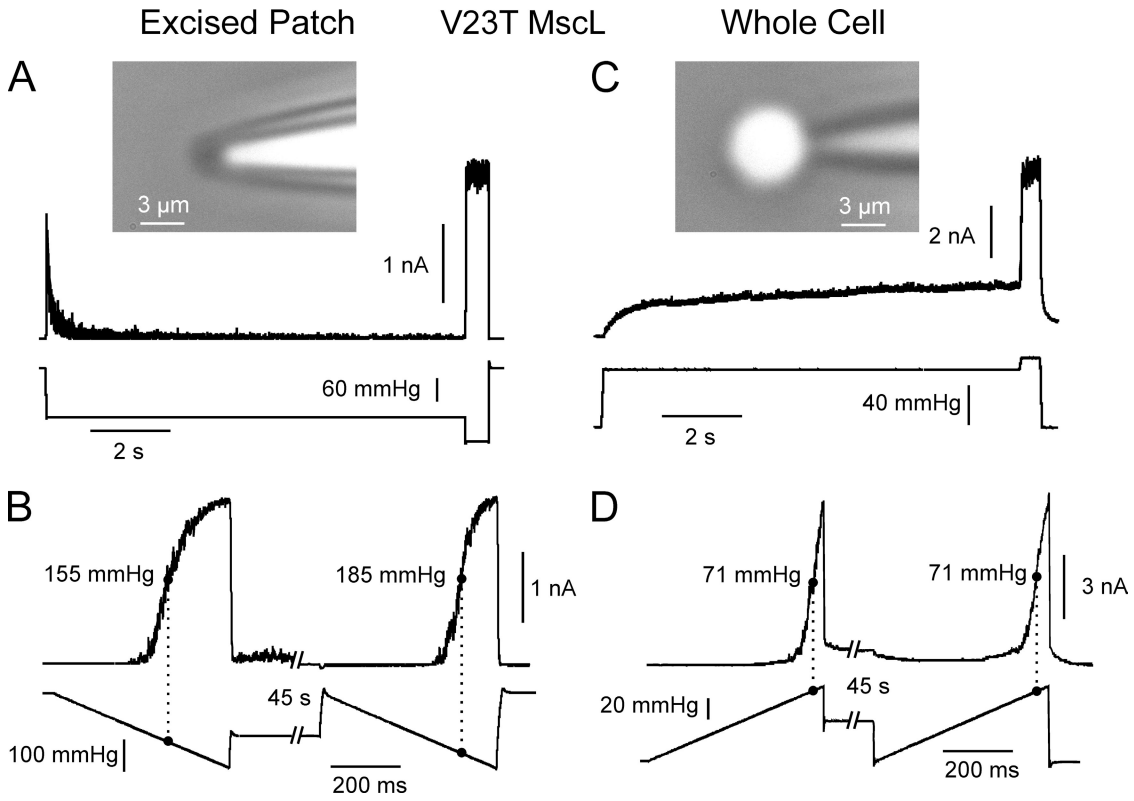

Figure 4. The MscL (V23T) channel quickly adapts in excised patches but shows no adaptation in whole cell mode. (A) Fast adaptation in response to a step of pressure in excised patch. (B) Responses to two ramps separated by a 45-s near-threshold conditioning pulse (ramp-step-ramp). The response to the second ramp is right-shifted by 30 mmHg. (C) Whole spheroplast response to a step shows no adaptation. (D) The ramp-step-ramp response of whole spheroplast indicates no midpoint shift.

Another notable feature of whole spheroplast recordings was a reproducible lag in MscS opening upon pressure application at intermediate pressures. Instead of opening immediately and then closing adaptively as typically observed in excised patches, MscS channels in whole spheroplasts open gradually, over the timescale of a few seconds, approaching a steady level (Fig. 3 B). Whole cell recordings have also revealed a complete absence of midpoint shift of the activation curve elicited by two pressure ramps separated by an extended (40-s) subthreshold stimulus (Fig. 3 D), whereas a characteristic shift was observed in excised patches stimulated by a similar protocol (Fig. 3 C). All of the above results were reproduced at least six times under both standard and symmetric (400 mM sucrose in the pipette) conditions, the latter experiment ruling out the possibility of an osmotic imbalance being responsible for the nonadaptive MscS behavior in whole spheroplasts.

MscL channels do not adapt in whole cell mode

We repeated the same experiment with MscL and found that, just as with MscS, adaptation was absent in whole cell mode. Because wild-type MscL activates at 1.8 times higher tension than MscS, we chose the V23T mild gain-of-function mutant of MscL (Anishkin et al., 2005) that activates at a considerably lower tension, similar to MscS. Fig. 4 A shows an excised patch response to a two-step protocol featuring fast adaptation. A ramp-step-ramp protocol applied to the same patch indicates a 30-mmHg midpoint shift in response to the second ramp after the conditioning 45-s subthreshold step (Fig. 4 B). In contrast, in whole spheroplast mode, we observed no adaptation under sustained step (Fig. 4 C) and no midpoint shift upon 45-s conditioning under constant tension (Fig. 4 D). Because the MscL-expressing spheroplasts were extremely fragile, we did not stretch them to attain complete current saturation, but used the saturation level determined in the two-step protocol (Fig. 4 C) to determine the midpoint. The two stimulating ramps and the respective partial ramp responses are completely superimposable.

Responses in the cell-attached mode depend on integrity of the spheroplast membrane

To test whether patch excision specifically confers adaptation to the channels, we stimulated MscS in spheroplast-attached patches with sustained steps. Without patch excision, spheroplasts 3–5 μm in size were very fragile and were often "sucked" into the pipette; however, we succeeded in testing eight spheroplasts. The character of response to a pressure step was found to depend on the spheroplast optical appearance in phase contrast. Three of the tested cells were "shiny" and five were "gray." Intact spheroplasts appear as shiny spheres in phase contrast, as they retain most of their intracellular components and have high refractive index (Fig. 5 A). Their responses showed approximately three times smaller unitary currents due to high series resistance (Fig. 5 A, inset) and no adaptation. Spheroplasts that appear gray are compromised because they lost some of the intracellular content through partial lysis. These spheroplasts were more flaccid; however, responses to pressure steps revealed adaptation that was obviously delayed compared with that in excised patches (Fig. 5 B). Therefore, it appears that loss of membrane integrity permits adaptation in patches stimulated by suction. This suggests that the presence of

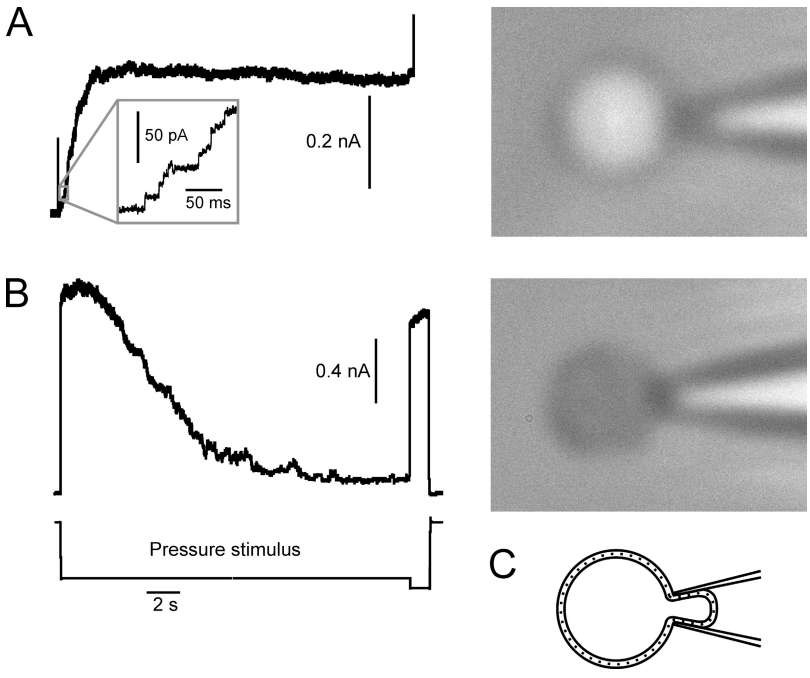

Figure 5. Responses of MscS in spheroplast-attached patches to a step stimulus. (A) Response of an intact "shiny" spheroplast shows no adaptive current decline. The phase-contrast appearance is different due to different gradients of refractive index across the membrane. Inset shows that unitary MscS currents (10 pA at −30 mV) appear three times smaller than in excised patches (30 pA) due to the series resistance of the spheroplast membrane. (B) Adaptive response of a "gray" partially lysed spheroplast. The character of adaptation is delayed compared with excised patches (Fig. 3 A). The figure represents typical responses out of five gray and three shiny spheroplasts tested. (C) A cartoon illustrating the spheroplast-attached configuration.

the membrane edge surrounding the excised patch or a leak pore somewhere else in the membrane connecting the two leaflets permits stress redistribution that leads to adaptation.

Imaging of spheroplasts sets the tension scale for activation

Recording MscS currents in whole spheroplast mode allowed us to determine the channel's midpoint tension by applying Laplace's law. The spheroplast's radius at the midpoint pressure ($p_{0.5}$) was determined by imaging under a given pressure gradient (see Materials and methods). After the patch was disrupted and the internal contents of the spheroplast had equilibrated with asymmetric bath and pipette solutions (400 mM sucrose in the bath but not in the pipette), spheroplasts typically shrank by ~5%. Shrinking was not observed under symmetric conditions with sucrose in bath and pipette. When saturating pressure was reached at the end of the ramp, the spheroplasts' apparent radii typically increased by 3.0 ± 1.2% (n = 6). The current responses to saturating ramps (Fig. 6) were individually corrected for the series resistance of the pipette determined at the end of each experiment, and pressure midpoints were obtained. Although the spheroplasts were specifically chosen to cover a range of sizes, the calculated tension midpoints clustered closely and yielded $\gamma_{1/2}$ = 7.85 ± 0.14 mN/m (n = 9). This is considerably higher than the previously reported midpoint tension, 5.5 mN/m, which was determined for reconstituted MscS in asolectin liposomes (Sukharev, 2002). This discrepancy is possibly due to different lipid composition in these membranes, high protein density in the cytoplasmic membrane (~50% by weight; Kander, 1996), and/or some remnants of the outer membrane/cell wall restraining the spheroplast expansion. Because whole spheroplasts are more fragile than excised patches, we were unable to directly measure wild-type MscL currents in whole spheroplast mode, as the cells typically rupture before reaching the required tension. However, based on the MscS midpoint and the ratio $p_{0.5}$MscL/$p_{0.5}$MscS of 1.86 (Fig. 2), the midpoint for wild-type MscL in spheroplasts could be estimated as ~14 mN/m, which is higher than the previously determined 11.8 mN/m in asolectin liposomes (Sukharev et al., 1999), the 8 mN/m measured in phosphatidylcholine, and the 13 mN/m in phosphatidylethanolamine

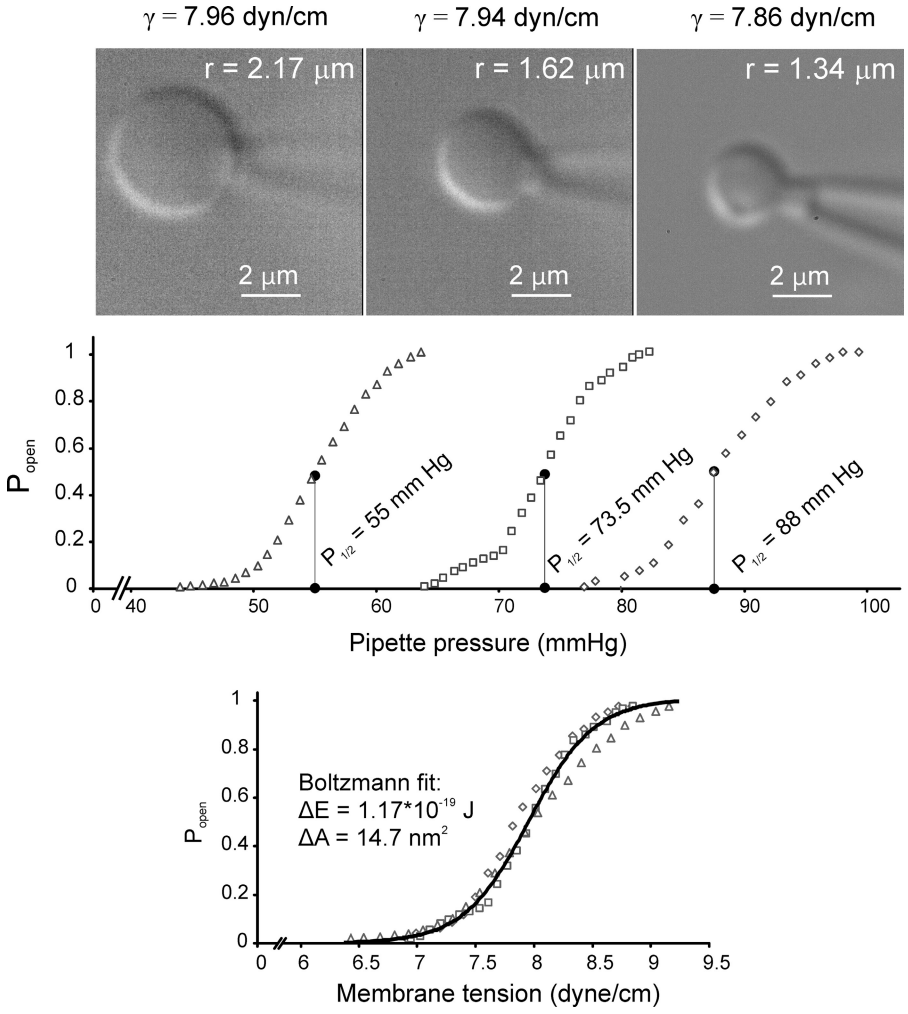

Figure 6. Whole spheroplast activation curves recorded with spheroplast imaging. (Top) Typical images of three spheroplasts of different sizes and their respective activation curves presented in the pressure scale. The fitting of the image was done using a custom-written MATLAB program. (Bottom) Curves from three spheroplasts presented in the tension scale. Tensions at each pressure were calculated according to Laplace's law for the sphere ($\gamma = p^*r/2$). The fit of the averaged curve to the Boltzmann-type equation (see Materials and methods) produces the values of $\Delta E = 1.17 \times 10^{-19}$ J (28 kT) and ΔA = 14.7 nm^2 (solid black line). The combined fit indicated average midpoint $\gamma_{0.5}$ = 7.8 mN/m.

liposomes (Moe and Blount, 2005). Triangular ramps of positive pressure applied to a spheroplast (Fig. S3) revealed the same hysteresis as in excised patches (compare with Fig. S2), illustrating MscS' slower closing rate in the whole cell configuration as well.

DISCUSSION

Here, we have compared two major mechanosensitive channels comprising the osmoprotective system in *E. coli* in patches excised from giant spheroplasts and in whole spheroplast mode. We show that adaptation is not unique to MscS, as similar stimulation protocols elicit nearly identical adaptive responses from the structurally unrelated channel MscL. Previously, adaptation of MscL was reported only in reconstituted liposomes (Häse et al., 1995). The fact that adaptation occurs simultaneously in MscS and MscL with similar shifts of their activation curves and identical time courses strongly suggests that this process may not reflect identical intrinsic properties in these channels, but rather an adaptation of the common stimulus. Again, based on the graded shift of activation curves, the tension-adapted state for neither channel appears to be a discrete conformational state. It was reported that the properties of the bilayer as a system of two coupled monolayers can affect mechanosensitive channels (Markin and Martinac, 1991; Perozo et al., 2002), and slippage of one leaflet relative to another can be a factor (Baoukina and Mukhin, 2004).

In contrast to *Lymnaea* neurons (Morris and Horn, 1991), it is possible to elicit whole cell mechanosensitive currents in patched yeast cells (Gustin et al., 1988), as well as in bacterial spheroplasts. Previous attempts of whole spheroplast recording yielded only partial activation curves (Cui et al., 1995; Cui and Adler, 1996). We succeeded in recording whole spheroplast MscS currents in a wide range of pressures, from threshold to saturation, and found no adaptation (Fig. 3). Likewise, we observed no adaptation of V23T MscL in whole spheroplast mode (Fig. 4). We also found no MscS adaptation in spheroplast-attached mode when the spheroplast membrane was intact, and observed delayed adaptation in leaky (compromised) spheroplasts (Fig. 5). We therefore propose that adaptation might be a result of lipid exchange between the leaflets through the edge of the disrupted membrane. Pressure may facilitate lipid redistribution and, as a result, tension redistribution between the inner and outer leaflets. It is especially pronounced in excised patches where the edge is closer to the active channels. Fig. 7 shows a cartoon depicting the force distribution across the excised patch inside the pipette under suction and across the spheroplast inflated with positive pressure through the pipette. In both configurations, only the outer membrane leaflet is sealed to the glass, whereas the inner leaflet, coupled to its counterpart through the common membrane midplane, may be free to slide. It seems plausible that in the whole cell configuration, internal pressure is distributed evenly across the free membrane area (i.e., the entire membrane outside the pipette), and that the minimum elastic energy case predicts equal strain and stress in both leaflets. This means that in the whole cell configuration, the distortion of the lateral pressure profile by tension would be symmetric, and the inner and outer rims of the channel would perceive roughly half of the total tension. When the excised patch is confined inside the pipette, the distribution of force is highly anisotropic and there is a predominant axial component in the direction of suction. The pressure forcing the patch into the pipette may promote a "rolling" of the membrane edge, taking lipids from the outer leaflet and putting them into the inner one. As a result, tension in the inner leaflet will relax. Because, according to Laplace, the total tension in a spherical patch should remain constant and equal to the pressure gradient times half-radius, larger tension will develop in the outer leaflet and reciprocally smaller tension in the inner leaflet. Viscous slippage of one leaflet along another can be a slow process dependent on the density and arrangement of integral proteins crossing the two leaflets and acting as obstacles. Indeed, with almost equal curvature signified by the same pressure midpoint ($p_{0.5}$), the characteristic adaptation time in our experiments varied within two orders of magnitude, indicating that the lipid exchange between the leaflets and the slippage may critically depend on the local conditions in the gigaseal zone (Suchyna et al., 2009), as well as on the distance between the channels and the membrane edge where the exchange may take place. Indeed, in compromised spheroplasts adaptation is delayed (Fig. 5), which is consistent with the idea that in this case the lipid exchange between the leaflets takes place farther away from active channels in the patch. Our observations show that in the absence of pressure, adaptation reverses with a characteristic time of ~200 ms to several seconds, depending on both the length and magnitude of the adaptation-inducing pressure step. We admit that lipid rearrangements under tension do not exclude mutual rearrangements in the protein, and for this reason we may infer silent transitions from the closed-resting state under 0 tension to a set of closed-adapted conformations under tension γ, but the shift of tension sensitivity appears to be largely lipid-borne.

The next question is why do both channels perceive the tension redistribution similarly by shifting the activation midpoint to the right by ~15%? In other words, why is the new distribution of tension after adaptation 15% less effective in driving the opening transition than an even distribution? At this moment we do not know what fraction of initial tension remains in the inner leaflet when adaptation saturates in ~30 s (Fig. 2 C), but

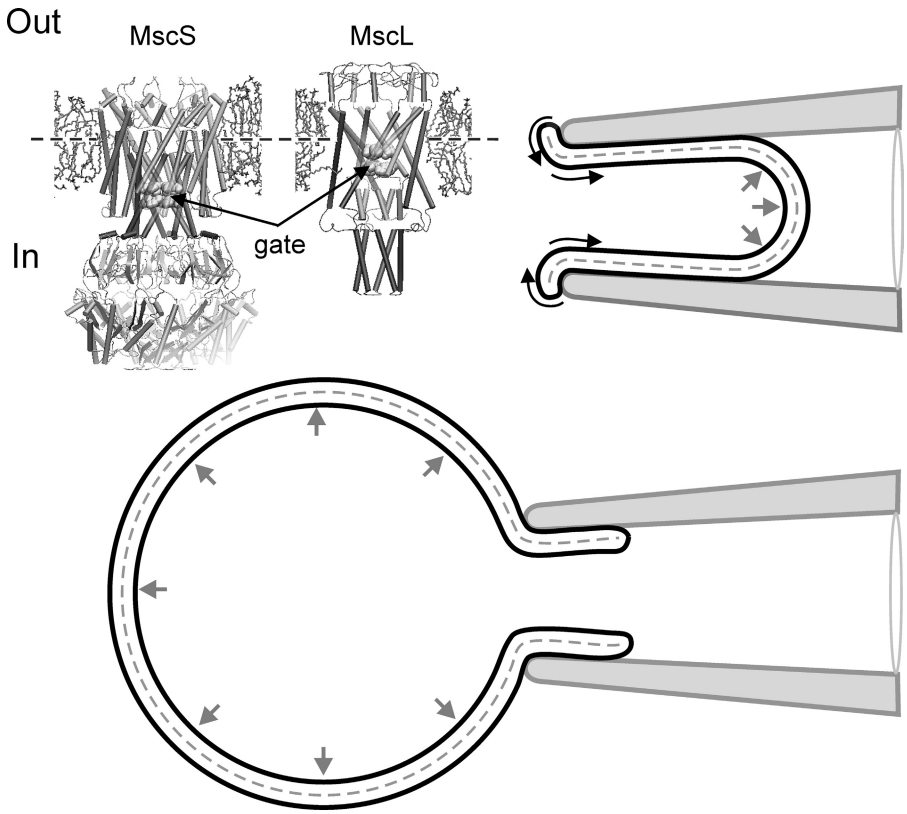

Figure 7. A cartoon illustrating relaxation of the inner leaflet of the membrane. The top right corner shows a configuration with an excised patch inside the pipette. Only the outer leaflet is in contact with the pipette, whereas the inner leaflet is free to relax. Anisotropic pressure gradient tends to promote "rolling" of the lipids across the membrane edge. The bottom panel shows whole spheroplast configuration with more isotropically distributed pressure. The molecular models illustrate cytoplasmic position of the gate in both channels relative to the membrane midplane (dashed line).

the structural design of MscL and MscS channels is such that the hydrophobic gate in both of them is located more cytoplasmically (Fig. 7, inset). Therefore, tension present in the inner leaflet is expected to be more effective in driving the transition. This paradigm of adaptation well corroborates with the previously reported increase of adaptation rate in the presence of amphipathic agents such as parabens (Kamaraju and Sukharev, 2008) and fluorinated alcohols (Akitake et al., 2007b). These amphipathic substances presented specifically from the cytoplasmic side of the patch shift MscS' activation curve to the right while strongly increasing the rate of adaptation. This can be explained by increased lateral pressure (opposing applied tension) and faster relaxation of tension due to time- and tension-dependent partitioning of these amphipaths from water into the inner leaflet.

Considering other factors that may potentially contribute to adaptation, we should mention change in membrane thickness or thickness mismatch (Perozo et al., 2002) and the effect of channel protein expansion ("spandex" effect) relieving part of membrane tension in closed cells (Boucher et al., 2009). The latter effect is expected to play a larger role at high density of channel expression in the membrane; however, we did not see any reproducible difference of the adaptation rate between non-induced (10–20 channels/patch) and induced (100–200 channels/patch) spheroplasts, as patch-to-patch variations in each type of preparation were large. The spandex effect would work in an intact cell, but in both excised patch and whole spheroplast configurations, tension γ is defined only by the pressure gradient Δp and radius of curvature r ($\gamma = \Delta pr/2$), so that tension is practically clamped and the spandex will not provide any significant relief. The opening of 100 MscS channels contributing $\sim$15 nm^2 each (Fig. 6) in a patch with r = 1 μm will increase the patch area only by 0.02%, and the small increase of patch radius is expected to slightly increase sensitivity, contrary to the decrease of sensitivity observed with adaptation.

Thickness mismatch does not seem to play a role either for the following reasons. We do not expect that there is any delay in small ($\sim$1–2%) thickness adjustment after tension application because isovolumic stretching and thinning of the bilayer should occur simultaneously. The difference in midpoint tension for MscL and MscS channels is about twofold, and membrane thinning accompanying MscL opening should be stronger. Yet, we see similar shifts and time courses of current relaxation for the two channels, suggesting that bilayer thickness may not be a defining factor. Thickness mismatch should take place in both whole spheroplast mode and excised patches, yet we see it only in the latter case. We cannot exclude that a delayed diffusional lipid rearrangement matching the thickness of an open channel may take place at the rim of the protein. In this case, shorter lipids recruited to the rim should alleviate the lipid compression stress, and this should stabilize the open state

shifting the activation curve to the left, not to the right. We rather conclude that the presence of membrane defects in leaky spheroplasts or free edges around excised patches leads to a stress redistribution through lipid exchange between the leaflets. This exchange takes place in patches confined in the pipette and can be assisted by anisotropic pressure distribution. The presented data show that adaptation of bacterial mechanosensitive channels is largely an artifact of patch excision. The results above also suggest that similar effects may take place in other systems where pressure is applied to excised patches. The differences in channel behavior between cell-attached and excised patches may occur not only due to the loss of cytoplasmic factors or cytoskeleton, but also due to a new pressure profile distribution and dynamics. With this regard, the effects of lipid flippases and scramblases that provide lipid exchange between the leaflets should also be considered as potential regulatory factors for membrane mechanisms of mechanosensation.

The authors thank Mrs. Naili Liu for technical assistance with spheroplast preparations.

This work was supported by the National Institutes of Health grants GM075225 and NS03931405A (to S. Sukharev) and an Howard Hughes Medical Institute undergraduate research fellowship provided through University of Maryland (to V. Belyy).

Lawrence G. Palmer served as editor.

Submitted: 3 December 2009
Accepted: 6 May 2010

REFERENCES

Akitake, B., A. Anishkin, and S. Sukharev. 2005. The "dashpot" mechanism of stretch-dependent gating in MscS. *J. Gen. Physiol.* 125:143–154. doi:10.1085/jgp.200409198

Akitake, B., A. Anishkin, N. Liu, and S. Sukharev. 2007a. Straightening and sequential buckling of the pore-lining helices define the gating cycle of MscS. *Nat. Struct. Mol. Biol.* 14:1141–1149. doi:10.1038/nsmb1341

Akitake, B., R.E. Spelbrink, A. Anishkin, J.A. Killian, B. de Kruijff, and S. Sukharev. 2007b. 2,2,2-Trifluoroethanol changes the transition kinetics and subunit interactions in the small bacterial mechanosensitive channel MscS. *Biophys. J.* 92:2771–2784. doi:10.1529/biophysj.106.098715

Anishkin, A., C.S. Chiang, and S. Sukharev. 2005. Gain-of-function mutations reveal expanded intermediate states and a sequential action of two gates in MscL. *J. Gen. Physiol.* 125:155–170. doi:10.1085/jgp.200409118

Baoukina, S.V., and S.I. Mukhin. 2004. Bilayer membrane in confined geometry: interlayer slide and entropic repulsion. *J. Exp. Theor. Phys.* 99:875–888. doi:10.1134/1.1826180

Blount, P., S.I. Sukharev, P.C. Moe, M.J. Schroeder, H.R. Guy, and C. Kung. 1996. Membrane topology and multimeric structure of a mechanosensitive channel protein of Escherichia coli. *EMBO J.* 15:4798–4805.

Blount, P., S.I. Sukharev, P.C. Moe, B. Martinac, and C. Kung. 1999. Mechanosensitive channels of bacteria. *Methods Enzymol.* 294:458–482. doi:10.1016/S0076-6879(99)94027-2

Boucher, P.A., C.E. Morris, and B. Joós. 2009. Mechanosensitive closed-closed transitions in large membrane proteins: osmoprotection and tension damping. *Biophys. J.* 97:2761–2770. doi:10.1016/j.bpj.2009.08.054

Cui, C., and J. Adler. 1996. Effect of mutation of potassium-efflux system, KefA, on mechanosensitive channels in the cytoplasmic membrane of Escherichia coli. *J. Membr. Biol.* 150:143–152. doi:10.1007/s002329900039

Cui, C., D.O. Smith, and J. Adler. 1995. Characterization of mechanosensitive channels in Escherichia coli cytoplasmic membrane by whole-cell patch clamp recording. *J. Membr. Biol.* 144:31–42.

Grajkowski, W., A. Kubalski, and P. Koprowski. 2005. Surface changes of the mechanosensitive channel MscS upon its activation, inactivation, and closing. *Biophys. J.* 88:3050–3059. doi:10.1529/biophysj.104.053546

Gustin, M.C., X.L. Zhou, B. Martinac, and C. Kung. 1988. A mechanosensitive ion channel in the yeast plasma membrane. *Science.* 242:762–765. doi:10.1126/science.2460920

Hamill, O.P., and B. Martinac. 2001. Molecular basis of mechanotransduction in living cells. *Physiol. Rev.* 81:685–740.

Hamill, O.P., and D.W. McBride Jr. 1992. Rapid adaptation of single mechanosensitive channels in Xenopus oocytes. *Proc. Natl. Acad. Sci. USA.* 89:7462–7466. doi:10.1073/pnas.89.16.7462

Häse, C.C., A.C. Le Dain, and B. Martinac. 1995. Purification and functional reconstitution of the recombinant large mechanosensitive ion channel (MscL) of Escherichia coli. *J. Biol. Chem.* 270:18329–18334. doi:10.1074/jbc.270.31.18329

Honoré, E., A.J. Patel, J. Chemin, T. Suchyna, and F. Sachs. 2006. Desensitization of mechano-gated K2P channels. *Proc. Natl. Acad. Sci. USA.* 103:6859–6864. doi:10.1073/pnas.0600463103

Kamaraju, K., and S. Sukharev. 2008. The membrane lateral pressure-perturbing capacity of parabens and their effects on the mechanosensitive channel directly correlate with hydrophobicity. *Biochemistry.* 47:10540–10550. doi:10.1021/bi801092g

Kander, R.J. 1996. Cytoplasmic membrane. *In* Escherichia coli and Salmonella: Cellular and Molecular Biology. F.C. Neidhardt, R. Curtiss III, J.L. Ingraham, E.C.C. Lin, K.B. Low, B. Magasanik, W.S. Reznikoff, M. Riley, M. Schaechter, and H.E. Umbarger, editors. ASM Press, Washington, DC. 58–87.

Koprowski, P., and A. Kubalski. 1998. Voltage-independent adaptation of mechanosensitive channels in Escherichia coli protoplasts. *J. Membr. Biol.* 164:253–262. doi:10.1007/s002329900410

Levina, N., S. Tötemeyer, N.R. Stokes, P. Louis, M.A. Jones, and I.R. Booth. 1999. Protection of Escherichia coli cells against extreme turgor by activation of MscS and MscL mechanosensitive channels: identification of genes required for MscS activity. *EMBO J.* 18:1730–1737. doi:10.1093/emboj/18.7.1730

Li, Y., P.C. Moe, S. Chandrasekaran, I.R. Booth, and P. Blount. 2002. Ionic regulation of MscK, a mechanosensitive channel from Escherichia coli. *EMBO J.* 21:5323–5330. doi:10.1093/emboj/cdf537

Markin, V.S., and B. Martinac. 1991. Mechanosensitive ion channels as reporters of bilayer expansion. A theoretical model. *Biophys. J.* 60:1120–1127. doi:10.1016/S0006-3495(91)82147-6

Moe, P., and P. Blount. 2005. Assessment of potential stimuli for mechano-dependent gating of MscL: effects of pressure, tension, and lipid headgroups. *Biochemistry.* 44:12239–12244. doi:10.1021/bi0509649

Morris, C.E., and R. Horn. 1991. Failure to elicit neuronal macroscopic mechanosensitive currents anticipated by single-channel studies. *Science.* 251:1246–1249. doi:10.1126/science.1706535

Okada, K., P.C. Moe, and P. Blount. 2002. Functional design of bacterial mechanosensitive channels. Comparisons and contrasts illuminated by random mutagenesis. *J. Biol. Chem.* 277:27682–27688. doi:10.1074/jbc.M202497200

Perozo, E., A. Kloda, D.M. Cortes, and B. Martinac. 2002. Physical principles underlying the transduction of bilayer deformation

forces during mechanosensitive channel gating. *Nat. Struct. Biol.* 9:696–703. doi:10.1038/nsb827

Sachs, F., and C.E. Morris. 1998. Mechanosensitive ion channels in nonspecialized cells. *Rev. Physiol. Biochem. Pharmacol.* 132:1–77. doi:10.1007/BFb0004985

Suchyna, T.M., and F. Sachs. 2007. Mechanosensitive channel properties and membrane mechanics in mouse dystrophic myotubes. *J. Physiol.* 581:369–387. doi:10.1113/jphysiol.2006.125021

Suchyna, T.M., S.R. Besch, and F. Sachs. 2004. Dynamic regulation of mechanosensitive channels: capacitance used to monitor patch tension in real time. *Phys. Biol.* 1:1–18. doi:10.1088/1478-3967/1/1/001

Suchyna, T.M., V.S. Markin, and F. Sachs. 2009. Biophysics and structure of the patch and the gigaseal. *Biophys. J.* 97:738–747. doi:10.1016/j.bpj.2009.05.018

Sukharev, S. 2002. Purification of the small mechanosensitive channel of Escherichia coli (MscS): the subunit structure, conduction, and gating characteristics in liposomes. *Biophys. J.* 83:290–298. doi:10.1016/S0006-3495(02)75169-2

Sukharev, S.I., W.J. Sigurdson, C. Kung, and F. Sachs. 1999. Energetic and spatial parameters for gating of the bacterial large conductance mechanosensitive channel, MscL. *J. Gen. Physiol.* 113:525–540. doi:10.1085/jgp.113.4.525

Vasquez, V., and E. Perozo. 2004. Voltage dependent gating in MscS. *Biophys. J.* 86:545A.

Wan, X., P. Juranka, and C.E. Morris. 1999. Activation of mechanosensitive currents in traumatized membrane. *Am. J. Physiol.* 276:C318–C327.

Young, D., C.A. Glasbey, A.J. Gray, and N.J. Martin. 1998. Towards automatic cell identification in DIC microscopy. *J. Microsc.* 192:186–193. doi:10.1046/j.1365-2818.1998.00397.x

Zhang, Y., F. Gao, V.L. Popov, J.W. Wen, and O.P. Hamill. 2000. Mechanically gated channel activity in cytoskeleton-deficient plasma membrane blebs and vesicles from Xenopus oocytes. *J. Physiol.* 523:117–130. doi:10.1111/j.1469-7793.2000.t01-1-00117.x